

## GRB BEAMING AND GRAVITATIONAL-WAVE OBSERVATIONS

HSIN-YU CHEN<sup>1</sup> AND DANIEL E. HOLZ<sup>2</sup>

<sup>1</sup>Department of Astronomy and Astrophysics, University of Chicago, Chicago, IL 60637

<sup>2</sup>Enrico Fermi Institute, Department of Physics, and Kavli Institute for Cosmological Physics  
University of Chicago, Chicago, IL 60637

*Draft version November 12, 2018*

### ABSTRACT

Using the observed rate of short-duration gamma-ray bursts (GRBs) it is possible to make predictions for the detectable rate of compact binary coalescences in gravitational-wave detectors. These estimates rely crucially on the growing consensus that short gamma-ray bursts are associated with the merger of two neutron stars or a neutron star and a black hole, but otherwise make no assumptions beyond the observed rate of short GRBs. In particular, our results do not assume coincident gravitational wave and electromagnetic observations. We show that the non-detection of mergers in the existing LIGO/Virgo data constrains the progenitor masses and beaming angles of gamma-ray bursts (e.g.,  $\theta_j > 4^\circ$  for  $M_{\text{total}} \geq 20M_\odot$ , for uniform component mass), although these limits are fully consistent with existing expectations. We make predictions for the rate of events in future networks of gravitational-wave observatories, finding that the first detection of a NS–NS binary coalescence associated with the progenitors of short GRBs is likely to happen within the first 16 months of observation, even in the case of a modest network of observatories (e.g., only LIGO-Hanford and LIGO-Livingston) operating at modest sensitivities (e.g., advanced LIGO design sensitivity, but without signal recycling mirrors), and assuming a conservative distribution of beaming angles (e.g. all GRBs beamed with  $\theta_j = 30^\circ$ ). Less conservative assumptions reduce the waiting time until first detection to a period of weeks to months. Alternatively, the compact binary coalescence model of short GRBs can be ruled out if a binary is not seen within the first two years of operation of a LIGO-Hanford, LIGO-Livingston, and Virgo network at advanced design sensitivity. We also demonstrate that the rate of GRB triggered sources is less than the rate of untriggered events if  $\theta_j \lesssim 30^\circ$ , independent of the noise curve, network configuration, and observed GRB rate. Thus the first detection in GWs of a binary GRB progenitor is unlikely to be associated with the observation of a GRB.

### 1. INTRODUCTION

The LIGO and Virgo collaborations have recently released results from roughly a half year of observations, investigating the gravitational wave (GW) sky at unprecedented levels of sensitivity (Abadie et al. 2012b). They did not identify any gravitational wave sources, and thereby established new upper limits on the rates of a variety of possible GW events in the nearby ( $< 200$  Mpc) Universe (Abadie et al. 2011). One of the most promising sources for GWs detectable by these ground-based observatories is the coalescence and merger of a compact binary system: two neutron stars (NS), two black holes (BH), or one of each.

There has been an active program of observing gamma-ray bursts (GRBs), focusing on rapid follow-up to determine afterglows and identify host galaxies (Soderberg et al. 2006; Panaitescu 2006; Berger et al. 2007; Perley et al. 2009). As a result, there is growing evidence that short/hard gamma-ray bursts are associated with the mergers of either two neutron stars, or a neutron star with a black hole (Fong et al. 2010; Church et al. 2011; Berger 2011). This consensus is based on noting that the physical timescales are commensurate, the short GRBs do not appear to be associated with star formation (and therefore are unlikely to be associated with supernovae), and the GRBs occur far from the centers of their host galaxies. These studies have also provided redshifts for a subsample of short GRBs, thereby providing preliminary estimates

for the rate densities of these events (Nakar et al. 2006; Dietz 2011). There is great interest in gravitational wave/electromagnetic multi-messenger observations of these GRBs (Metzger & Berger 2012; Evans et al. 2012; Briggs et al. 2012), as such systems would help confirm the first detections of GWs, elucidate the properties of GRBs, and potentially provide interesting measurements of the Hubble constant and the dark energy equation-of-state (Schutz 1986; Holz & Hughes 2005; Dalal et al. 2006; Nissanke et al. 2010).

One of the most important properties of GRBs is the beaming of the gamma rays. This beaming directly relates to the total electromagnetic energy of the explosion, as well as the intrinsic event rate of the sources (as compared to the observed rate, which is a function of the ones that happen to point at us). Recent observations of a jet break in the short-duration gamma-ray burst GRB 111020A suggests a beaming opening angle of  $\theta_j \sim 3\text{--}8^\circ$  (Fong et al. 2012). Other GRBs (e.g., GRB 070714B, GRB 070724A, and GRB 071227) have been found with beaming angles in the range  $1\text{--}30^\circ$  (Fong et al. 2012; Coward et al. 2012), while non-detection of a jet break in the light curve of GRB 050724A places a lower limit on the beaming of that burst of  $\theta_j \geq 25^\circ$  (Grupe et al. 2006). Numerical studies, on the other hand, find  $\theta_j \leq 30^\circ$  (Popham et al. 1999; Rosswog & Ramirez-Ruiz 2002; Janka et al. 2006; Rezzolla et al. 2011).

In this paper we estimate the limits that arise on

the beaming of short-duration GRBs based on the non-detection of GWs from associated binary systems in the recent LIGO/Virgo science run. We also make projections for the detection rate of binary systems, as a function of mass and beaming angle, for future networks of GW observatories. We take a conservative lower limit on the observed rate density of local short GRBs of  $\mathcal{R}_{\text{GRB}} = 10 \text{ yr}^{-1} \text{ Gpc}^{-3}$  (Nakar et al. 2006; Dietz 2011; Coward et al. 2012), based primarily on BATSE and *Swift* observations. We emphasize that this rate is determined purely through observations, although it is broadly consistent with the rates arising from population synthesis (Belczynski et al. 2006; O’Shaughnessy et al. 2008; Belczynski et al. 2010; Abadie et al. 2010; Dominik et al. 2012). The gravitational-wave limits presented here are based on observed GRB rates, and are therefore independent of, and complementary to, estimates based on population synthesis modeling.

We assume that all short GRBs are associated with low-mass compact binary coalescence. There is developing evidence that this is the case, with perhaps a small sample of nearby GRBs occurring from other mechanisms, such as flares from soft gamma repeaters (Levan et al. 2008; Abbott et al. 2008). While it is conceivable that not all short GRBs are the result of binary coalescences, it is perhaps even more likely that not all binary coalescences result in GRBs. We thus expect that our limits on the minimum beaming angle in Sec. 2 are low, and our estimates of the maximum wait time in Sec. 3 are high.

## 2. LIGO S6/VIRGO VSR2

From July 2009 to October 2010 the LIGO and Virgo observatories conducted a search (S6/VSR2–3) for compact binary coalescences (Abadie et al. 2011, 2012a,b). They did not detect any gravitational-wave events, and thereby established upper limits on the event rates of coalescences in the local Universe (Abadie et al. 2011). The LIGO instruments operating during S6 were the 4 km laser interferometers at Hanford, WA [H] and Livingston, LA [L], while the Virgo [V] results were from a single 3 km laser interferometer in Cascina, Italy. The S6/VSR2 runs consisted of 0.09 years of HLV coincident data, 0.17 years of HL, 0.10 years of HV, and 0.07 years of LV.<sup>1</sup>

We have taken the representative sensitivities presented in Fig. 1 of Abadie et al. (2011), and calculated the corresponding horizon distances,  $R_0$ , for H, L, and V, where horizon distance is defined to be the distance at which a given signal-to-noise (SNR),  $\rho$ , is measured for an optimally oriented (face-on) and optimally located (directly overhead) binary. From Dalal et al. (2006):

$$R_0 = 4\mathcal{A}\sqrt{I_7}/\rho, \quad (1)$$

where  $\mathcal{A} = \sqrt{5/96}\pi^{-2/3}(GM/c^3)^{5/6}c$ , and where the binary chirp mass is given by  $\mathcal{M} = (m_1 m_2)^{3/5}/(m_1 + m_2)^{1/5}$ . In this paper we are only interested in nearby sources ( $z < 0.2$ ), and for simplicity neglect the redshift

<sup>1</sup> Due to compromised sensitivity from the installation of an incorrect mirror, we follow Abadie et al. (2011) in removing the Virgo SR3 data from our analysis.

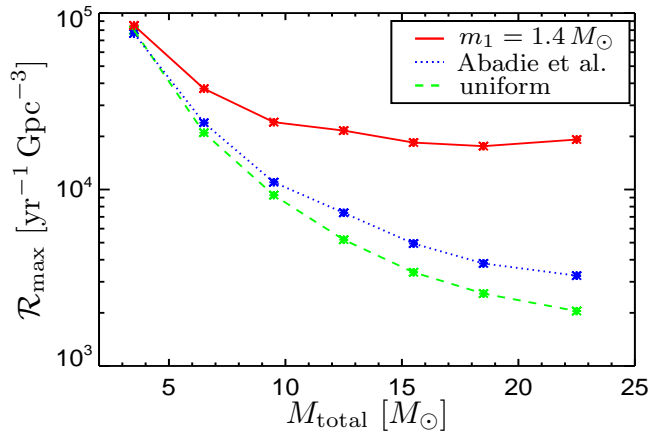


FIG. 1.— Maximum rate density of binary coalescences as a function of total mass of the binary, given the non-detection of any binary systems in the LIGO/Virgo S6/V2 observing runs. The dotted blue curve is the result from Fig. 4 of Abadie et al. (2011), setting an upper limit on the rate density, where each mass bin is averaged over a uniform distribution of component masses. The dashed green curve shows our result for this curve, where we have assumed a fixed SNR network threshold of  $\rho = 9.4$ . The lower sensitivity of the Abadie curve at higher mass is due to non-stationary noise. We calculate an effective SNR network threshold, as a function of mass, to match the Abadie curve, and we use this to calculate the equivalent curve assume that  $m_1 = 1.4 M_\odot$  (i.e., that the NS mass is fixed, and the black hole mass is given by  $m_2 = M_{\text{total}} - 1.4$ ).

dependence of the chirp mass (Holz & Hughes 2005). The characteristics of the detector are encapsulated in

$$I_7 = \int_{f_{\text{low}}}^{f_{\text{high}}} \frac{f^{-7/3}}{S_h(f)} df, \quad (2)$$

with  $S_h(f)$  the noise spectral density of the detector. We follow the approach of LIGO’s compact binary coalescence searches (Abadie et al. 2012b), and take  $f_{\text{low}} = 40$  Hz for the LIGO detectors, and  $f_{\text{low}} = 50$  Hz for Virgo, with upper limits set by the frequency of the innermost stable circular orbit. To calculate the waveform we assume the members of the binary are non-spinning, and make use of the stationary phase approximation (Dalal et al. 2006; Abadie et al. 2012b).

We follow the approach of Schutz (2011) to combine the antenna patterns of the three different interferometers (HL, HV, LV, and HLV), taking into account the differing horizon distances (which are a function of the masses of the binary) as well as power patterns. The network weighted antenna power pattern, from eqs. (15)–(20) of Schutz (2011), is given by:

$$P_N(\theta, \phi) \equiv \sum_{k=1}^N ((F_{+,k}^2(\theta, \phi, \psi) + F_{\times,k}^2(\theta, \phi, \psi)) \rho_{\text{min},k}^2 R_{0,k}^2), \quad (3)$$

where  $F_{+,k}^2(\theta, \phi, \psi)$  and  $F_{\times,k}^2(\theta, \phi, \psi)$  are the antenna patterns for the  $k$ th detector, and  $\rho_{\text{min},k}$  and  $R_{0,k}$  are the SNR threshold and horizon distances of that detector, respectively. The detection distance for a network is related to the antenna pattern:  $R(\theta, \phi) = \sqrt{P_N(\theta, \phi)}/\rho_{\text{min}}$ , where  $\rho_{\text{min}}$  is the network signal-to-noise threshold. The sensitivity also depends upon the orientation of the binary; integrating over all orientations results in a factor of 0.29 decrease in the mean detectable

volume (Sathyaprakash & Schutz 2009; Schutz 2011):

$$\bar{V} = \frac{0.29}{3} \frac{1}{\rho_{\min}^3} \int P_N^{3/2}(\theta, \phi) d\Omega. \quad (4)$$

Since the LIGO/Virgo network did not detect any gravitational wave sources during its last science run, we can combine all network configurations and corresponding coincident observational times to estimate a 90% upper limit to the rate density:  $\mathcal{R} = 2.3/(\sum_i \bar{V}_i \times \Delta t_i)$ , where the sum is over the different detector networks configurations,  $\Delta t_i$  is the amount of observational time for network configuration  $i$ , and the factor of 2.3 is in accordance with a Poisson process (see the discussion below eq. 6). We plot our results in Fig. 1, assuming a combined network threshold of  $\rho = 9.4$ . This is to be compared with Fig. 4 of Abadie et al. (2011), which calculates the same quantity through detailed analysis of the GW data stream from the LIGO and Virgo instruments (Brady et al. 2004). We have tuned our SNR threshold to agree for low mass binaries, but our results begin to deviate at higher mass ( $M_{\text{total}} \gtrsim 10 M_{\odot}$ ), since the signal shifts to lower frequencies and is therefore more sensitive to non-stationary noise in the detectors (in part because there are fewer cycles to integrate against). To get a sense of the importance of this effect, we calculate the effective network SNR threshold which we would need to apply, as a function of mass, to match the rate limits which come out of the full analysis presented in Abadie et al. (2011). From a value of  $\rho = 9.4$  at  $M_{\text{total}} = 3.5 M_{\odot}$ , the non-stationary noise degrades the sensitivity of the instruments at higher masses, leading to  $\rho = 10.7$  at 11–14  $M_{\odot}$ , and  $\rho = 11.1$  at 20–25  $M_{\odot}$ . In what follows we incorporate this mass dependence into our effective SNR thresholds. We note that Abadie et al. (2011) assume a uniform distribution of component masses for their binaries. We also consider the case where the neutron star is restricted to have  $m_1 = 1.4 M_{\odot}$ , and the mass of the companion is given by  $m_2 = M_{\text{total}} - m_1$ . Because this entails higher mass ratios for higher mass binaries, it decreases the overall gravitational-wave strength of the sources in comparison to the uniform distributions, and therefore decreases the detectable volume. As can be seen in Fig. 1, this results in a negligible effect at low mass, but rises to a factor of 3.6 in the rate at  $M_{\text{total}} = 15 M_{\odot}$  and 6.8 at  $M_{\text{total}} = 25 M_{\odot}$ .

We define the beaming angle,  $\theta_j$ , to be the half opening angle of one of the two polar jets of a gamma-ray burst. The fraction of the sky,  $f_b$ , covered by the beamed gamma rays is given by  $f_b = 1 - \cos\theta_j$ . Given the paucity of data on the beaming of short GRBs, it is premature to assume knowledge of the distribution of beaming angles. We therefore will assume that all short GRBs have a fixed beaming angle,  $\theta_j$ , with the understanding that this fixed angle provides the same results as the appropriate average of the true distribution of beaming angles. In other words,  $1/(1 - \cos\theta_j) \equiv \int P(\theta)/(1 - \cos\theta) d\theta$ , where  $P(\theta)$  is the true distribution of beaming angles. Assuming all short GRBs have compact binary progenitors, the implied rate density of these coalescences is given by  $\mathcal{R} = \mathcal{R}_{\text{GRB}}/f_b = \mathcal{R}_{\text{GRB}}/(1 - \cos\theta_j)$ . If only a fraction,  $f_{\text{CBC}}$ , of short GRBs result from compact binary coalescence, then the rate density becomes

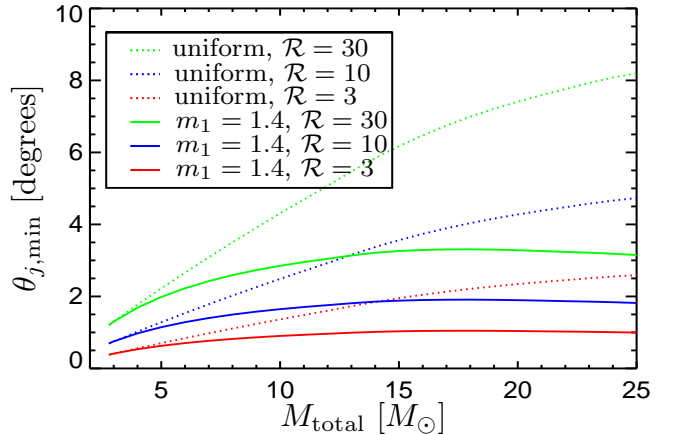


FIG. 2.— Minimum beaming half-angle,  $\theta_{j,\min}$ , as a function of the total mass of the binaries. We plot results for three different rates of short GRBs,  $\mathcal{R} = 3, 10$ , and  $30 \text{ yr}^{-1} \text{ Gpc}^{-3}$ , and for two different distributions ( $m_1$  is uniform from 1 to  $M_{\text{total}}$ , and  $m_1 = 1.4 M_{\odot}$ ). Given the lack of detection of binaries in LIGO/Virgo S6/V2, the beaming angles of short GRBs will be greater than what is plotted in 90% of cases. We use a network threshold which matches the Abadie et al. (2011) results (see text for details).

$\mathcal{R} = f_{\text{CBC}} \mathcal{R}_{\text{GRB}} / (1 - \cos\theta_j)$ . In Fig. 2 we plot the 90% lower limit on the beaming angle as a function of the mass of the progenitors. We take the observed rate of short GRBs to be 3, 10, or  $30 \text{ yr}^{-1} \text{ Gpc}^{-3}$  (Nakar et al. 2006; Guetta & Stella 2009; Coward et al. 2012). For example, a rate of  $3 \text{ yr}^{-1} \text{ Gpc}^{-3}$  can be thought of as a very conservative estimate of  $\mathcal{R} = 2 \text{ yr}^{-1} \text{ Gpc}^{-3}$  with a very conservative estimate of  $f_{\text{CBC}} = 0.5$ . This simple analysis suggests that models of short GRBs with progenitors of mass  $M_{\text{total}} > 20 M_{\odot}$  (uniformly distributed in component mass) and with a beaming angle  $\theta_j < 4^\circ$  are inconsistent with existing LIGO/Virgo data. This weakens significantly for more realistic masses and mass ratios, with a minimum beaming angle of  $\sim 1^\circ$  at  $M_{\text{total}} \sim 3 M_{\odot}$ . These limits are completely consistent with observations and expectations. The current LIGO/Virgo data is on the verge of providing interesting astrophysical constraints, which suggests that the next generation of detectors should provide quick detections, or alternatively, the lack of quick detections would provide strong lower limits on the beaming of short GRBs. We explore these constraints in the next section.

### 3. ADVANCED LIGO/VIRGO

We now calculate the expected detection rate of short GRB progenitors in the advanced LIGO and Virgo detectors, as well as additional detectors in Japan (KAGRA)<sup>2</sup> and India (IndIGO)<sup>3</sup>. The advanced LIGO detectors are expected to begin operation in  $\sim 2015$ , and it is hoped that the LIGO and Virgo observatories will achieve their target advanced detector sensitivities by  $\sim 2017$ , with the Japanese [J] and Indian [I] detectors operating at comparable sensitivities by  $\sim 2020$ . We assume an identical noise curve for each of these instruments, given by the representative advanced LIGO noise curves in LIGO document T0900288-v3,<sup>4</sup> with

<sup>2</sup> gwcenter.icrr.u-tokyo.ac.jp/en/

<sup>3</sup> www.gw-indigo.org/tiki-index.php

<sup>4</sup> dcc.ligo.org/cgi-bin/DocDB/ShowDocument?docid=2974

Network	$V_0(\text{Gpc}^3)$	$T_{\text{first}}$	$\theta_j = 10^\circ$	$\theta_j = 30^\circ$	$\theta_j = 90^\circ$
HL(no SRM)	0.027	1.00	1.8	16	120
HLV(no SRM)	0.046	0.59	1.1	9.4	70
HLV	0.092	0.31	0.56	4.9	37
HLVJ	0.14	0.21	0.37	3.3	25
HLVI	0.14	0.20	0.36	3.2	24
HLVJI	0.19	0.15	0.27	2.3	17

TABLE 1

MEAN DETECTABLE VOLUME AND WAIT TIMES FOR THE DETECTION OF BINARY COALESCENCE ASSOCIATED WITH SHORT GRBs IN FUTURE GW DETECTOR NETWORKS. THE NETWORK SNR IS TAKEN TO BE 10, AND THE VOLUME IS CALCULATED FOR A  $1.4 M_\odot$ – $1.4 M_\odot$  BINARY.  $T_{\text{first}}$  IS THE WAITING TIME UNTIL FIRST DETECTION, SCALED TO THE VALUE FOR THE HL NETWORK WITH THE “NO SRM” NOISE CURVE. THE LAST THREE COLUMNS LIST THE 90% WAIT TIME FOR FIRST DETECTION (IN MONTHS) FOR THREE DIFFERENT VALUES OF THE BEAMING ANGLE.

$f_{\text{low}} = 10 \text{ Hz}$ . We take the target design sensitivity to be given by the `ZERO_DET_high_P.txt` curve, corresponding to zero-detuning of the signal recycling mirror, and high laser power. We also consider an early, less sensitive incarnation of the detectors resulting from the absence of signal recycling mirrors, given by the `NO_SRM.txt` curve. It is possible that in 2015 the worldwide GW detector network will consist solely of HL in this lower sensitivity configuration.

We calculate the mean detectable volume,  $\bar{V}$ , of a variety of ground-based networks. Our results are presented in Table 1, where in all cases we have assumed a network SNR threshold of  $\rho = 10$ , and our sources are taken to be equal-mass binaries with  $m_1 = m_2 = 1.4 M_\odot$ . The mean detectable volume of a network is expected to scale as  $\mathcal{M}^{5/2}$  (see eqs. (1), (3), and (4)), although this relation is imperfect, since the scaling also depends on the shape of the noise curve. We fit the mass dependence to the functional form

$$\bar{V}(M_{\text{total}}) = V_0 \left( \frac{M_{\text{total}}}{2.8 M_\odot} \right)^p, \quad (5)$$

where  $V_0$  is the detection volume for a binary with  $M_{\text{total}} = 2.8 M_\odot$ , and we follow the previous section and fix  $m_1 = 1.4 M_\odot$  and  $m_2 = M_{\text{total}} - m_1$ . The “no SRM” noise curve yields  $p = 1.39$ , while our fiducial advanced LIGO noise curve yields  $p = 1.30$ . These fits are good to 20% at  $M_{\text{total}} = 30 M_\odot$ .<sup>5</sup>

We are interested in how quickly networks of advanced ground-based gravitational-wave detectors can be expected to see their first binary coalescences associated with short GRB progenitors. This rate is a function of the rate of observed GRBs (in gamma rays),  $\mathcal{R}_{\text{GRB}}$ , the sensitivity and configuration of the detectors, the mass distribution of the GRB progenitors, and the beaming of the GRBs. The event rate of detectable binaries for a network of GW observatories is given by

$$\lambda = \bar{V}(M_{\text{total}}) \mathcal{R}_{\text{GRB}} f_{\text{CBC}} / (1 - \cos \theta_j). \quad (6)$$

How long will a given network have to wait before seeing its first event? This is described by a Poisson process,

<sup>5</sup> For completeness, we also mention results for the `ZERO_DET_low_P.txt` noise curve, corresponding to a lower laser power. We find  $V_0 = 0.02 \text{ Gpc}^3$  for HL (no SRM),  $V_0 = 0.034 \text{ Gpc}^3$  for HLV, and  $p = 1.37$ .

with the probability of waiting a time  $\tau$  before detecting the first event given by  $e^{-\tau\lambda}$ . We define  $t_{\text{first}}$  as the waiting time by which, in 90% of cases, the first event will have been observed:  $t_{\text{first}} = -\ln(0.1)/\lambda = 2.3/\lambda$ . In Fig. 3 we plot  $t_{\text{first}}$  as a function of the beaming angle,  $\theta_j$ , for the HL and HLV networks. If one is interested in the waiting time by which the first event has been seen in 50% or 99% of the cases, the 90% waiting times are multiplied by 0.3 or 2, respectively. We have assumed  $f_{\text{CBC}} \times \mathcal{R}_{\text{GRB}} = 10 \text{ yr}^{-1} \text{ Gpc}^{-3}$ , and we have considered NS-NS equal mass binaries, with  $m_1 = m_2 = 1.4 M_\odot$ . We do not employ the mass-dependent threshold correction factors from the S6/V2-3 analysis derived in the previous section, since it can be argued that the non-stationary noise is less likely to be a problem in the advanced configuration of these detectors,<sup>6</sup> and, regardless, the functional form would not *a priori* be expected to match that of the lower sensitivity detectors. The representative curves in Fig. 3 can be rescaled to other parameter values of interest. For example, if either  $\mathcal{R}_{\text{GRB}}$  or  $f_{\text{CBC}}$  is down by a factor of 10, then the waiting times,  $t_{\text{first}}$ , are all multiplied by the same factor of 10. A change in the network configuration similarly results in an overall shift in the expected rates, and therefore an overall shift in  $t_{\text{first}}$ . The relative waiting times for other networks,  $T_{\text{first}}$ , are presented in Table 1, scaled to the HL (no SRM) value. The HLVJI network, with all detectors at the advanced zero-detuning high laser power sensitivity, has a waiting time that is a factor of 0.15 that of the HL (no SRM) curve, independent of the beaming angle. If we consider larger mass systems, the waiting time is correspondingly shortened (see eqs. (5) and (6)). For example, if we consider NS-BH systems, with  $M_{\text{NS}} = 1.4 M_\odot$  and with  $M_{\text{BH}} = 10 M_\odot$  and  $20 M_\odot$ , then the waiting times until first detection are a factor of 0.11 and 0.05 shorter than those for the NS-NS case presented in Fig. 3. It is to be noted that our results are roughly consistent with the completely independent rate estimates from population synthesis and observed binary pulsars (Abadie et al. 2010).

Alternatively, the binary origin of short GRBs can be falsified (at the 90% Poisson confidence discussed above) if no coalescences are observed with a full network (HLV) operating at design sensitivity (zero-detuning high laser power) over a period of 3 years. This limit comes from taking  $\theta_j = 90^\circ$ , which corresponds to none of the GRBs being beamed (which is already inconsistent with observations). If we take a conservative upper limit of  $\theta_j = 45^\circ$ , we find that the binary origin can be falsified (at the 99% level) in 70 months for HL (no SRM), and in 22 months for HLV. However, even if short GRBs are not the result of binary mergers, we nonetheless expect a population of merging systems, and these should be observable by future observatories (Abadie et al. 2010).

The predicted event rates for the various networks are related to the 90% waiting times by a factor of 2.3. If an HL network, using conservative noise curves (no SRM), takes 16 months before a first detection assuming a binary of mass  $1.4 M_\odot$ – $1.4 M_\odot$  and a beaming angle of  $\theta_j = 30^\circ$  (see Table 1), then the predicted event rate for this network is  $2.3/1.33 \text{ yr} = 1.7 \text{ yr}^{-1}$ . These results

<sup>6</sup> Peter Shawhan, private communication.

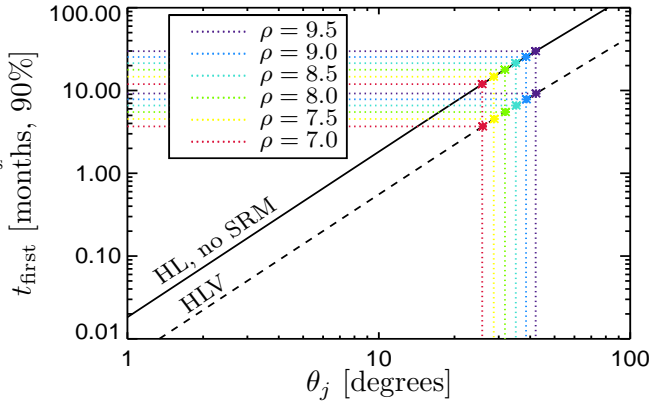


FIG. 3.— Waiting time until first detection,  $t_{\text{first}}$ , as a function of the beaming angle,  $\theta_j$ . Results are shown for both untriggered and triggered GW observations of GRB progenitors, where we have assumed the observed local short GRB rate is  $\mathcal{R}_{\text{GRB}} = 10 \text{ yr}^{-1} \text{ Gpc}^{-3}$ . In 90% of cases the waiting time will be less than the values indicated. We plot results for two different GW networks: Hanford+Livingston, operating without a signal recycling mirror (a potential early version of advanced LIGO) and Hanford+Livingston+Virgo, operating at the design sensitivity (at high laser power). Even in the pessimistic case (HL, no SRM, all short GRBs are beamed with  $\theta_j = 30^\circ$ ), the first untriggered binary detection is expected in less than 16 months. For more substantial GW networks, the expected wait time may be less than a month (e.g., if  $\theta_j \sim 10^\circ$ ). The dotted lines show the wait times for GRB triggered GW observations, for a range of values of  $\rho$ . The GRB trigger provides a time and sky position, thereby reducing the required SNR threshold and increasing the detection rate because the sources are assumed to be face-on. On the other hand, the triggering GRB rate is given by the  $\theta_j = 90^\circ$  values, and is not enhanced by beaming. The dotted lines show the equivalence beaming angles, at which the rates of triggered and untriggered GW observations of GRBs match each other; this is found to happen at  $\theta_j \sim 30^\circ$  for  $\rho \sim 7.5$ . For lower values of  $\theta_j$ , untriggered observations occur more frequently than those triggered by GRBs, and the first observed binary GRB progenitor will be seen first (and perhaps only) in GWs.

are consistent with those of Coward et al. (2012).

#### 4. TRIGGERED VERSUS UNTRIGGERED

An important question when considering the future GW detection of short GRBs is whether triggered or untriggered detections are more likely. A short GRB trigger improves the sensitivity of the GW search by reducing the need to marginalize over all times and sky positions. In addition, because the gamma-rays are thought to be beamed, a GRB trigger is expected to be face-on, thereby increasing the signal in GWs over a source with a random inclination. In other words, the strongest GW emitters happen to also be the ones observable in gamma-rays. A GW network is therefore substantially more sensitive to a GRB triggered source. On the other hand, for small beaming angles the rate density of GRB progenitors increases (approaching  $\infty$  as  $\theta_j \rightarrow 0$ ). For sufficiently small  $\theta_j$  the untriggered GW detection of a GRB progenitor will dominate over a triggered GRB, even considering the additional sensitivity in the latter case. We are interested in establishing whether triggered or untriggered GRBs are more likely for upcoming networks of GW observatories.

We have calculated the waiting time and event rates for untriggered observations of GRB progenitor systems above. We now consider the equivalent calculation in the case of a GRB trigger. We assume that the GRB is face-on, which improves the sensitivity of the net-

work by a factor of  $1/0.29$  (see eq. (4)). We now estimate the reduction in SNR threshold due to the known time and sky position of the source (Dalal et al. 2006). We assume  $\exp(-\rho^2/2) \propto 1/\#$  of templates, where in the untriggered case we took  $\rho = 10$ . If we take this threshold to have been based on roughly one year of observation, the existence of a GRB trigger now reduces the observational window down to  $\sim 10$  sec, for a reduction in the number of templates by a factor of  $\sim 10^6$ . If the sky localization in the untriggered case is  $\sim 5$  deg (Nissanke et al. 2011), then compared to a full-sky search ( $41,253 \text{ deg}^2$ ), the reduction in number of templates is a factor of  $\sim 10^3$ . The total number of templates is down by a factor of  $10^9$ , which for the equivalent false alarm rate would imply that the SNR threshold is reduced to  $\rho \sim \sqrt{-2 \log(\exp(-10^2/2) \times 10^9)} = 7.7$ .

In Fig. 3 we compare the wait times for untriggered and triggered GRBs. We find that the wait time for a triggered GRB is equivalent to the untriggered case if the average GRB beaming angle is  $\theta_j \sim 30^\circ$ . This result is independent of the network configuration, the individual noise curves, and the assumed GRB rate, and is weakly dependent on the specific value of the threshold improvement due to the reduced number of templates. If the GRBs have an average beaming value of  $\theta_j = 20^\circ$ , we would predict the rate of untriggered GRBs to be roughly double that of triggered ones. This increases to a factor of 10 if  $\theta_j = 10^\circ$ . Alternatively, the rates are equal if  $\theta_j = 30^\circ$ , and triggered GRBs are found at double the rate of untriggered ones if  $\theta_j = 45^\circ$ . It is to be noted that this process can be inverted, and the wait time before first detection (and in between the first few detections) may be used to infer the beaming angle of GRBs. In addition, the relative rates of triggered and untriggered GRBs will help establish the beaming, and will be an important test of consistency when compared with explicit determinations of the beaming distribution based on GW measurements of the inclination of GRB sources.

As discussed in Sec. 1, recent observations have measured short GRBs with  $\theta_j \sim 10^\circ$ , indicating that it is likely that the rate of untriggered GRBs will be greater than the rate of triggered ones, and implying that the first detection of a binary system which is a progenitor of a short GRB will not be triggered by a GRB. Although triggered GRBs may be less frequent than untriggered ones, multi-messenger observations of these systems holds tremendous scientific potential, and should be aggressively pursued (Bloom et al. 2009). Furthermore, the increase in psychological confidence of detection given coincident observation may play a large role in the initial detections. It is to be emphasized that our triggered rates assume the existence of an all-sky short GRB monitor operating contemporaneously with advanced GW networks.

#### 5. DISCUSSION

We have explored the connection between the observed short GRB rate, the beaming angle of short GRBs, and the predicted rate of detectable binary systems associated with progenitors of GRBs in networks of gravitational-wave observatories.

We have shown that existing LIGO/Virgo data pro-

vides preliminary constraints on the beaming angle and mass distribution of short GRB progenitor systems. For example, we find that short GRB progenitors of mass  $M_{\text{total}} > 20 M_{\odot}$  (uniformly distributed in component mass) and with beaming angles of  $\theta_j < 4^\circ$  are ruled out by existing LIGO/Virgo data. These constraints, while novel, are fully consistent with our current understanding of the short GRB engine and rates.

We have analyzed the observed rate of short GRB progenitors in future networks of GW detectors. We find that, even in the pessimistic case of only two detectors (HL) operating at conservative sensitivity (without a signal recycling mirror), in 90% of cases we would expect a first detection of a binary within 16 months if the GRBs are beamed within  $\theta_j = 30^\circ$ , and within 55 days if  $\theta_j = 10^\circ$ . The expected event rates are  $1.7 \text{ yr}^{-1}$  ( $\theta_j = 30^\circ$ ) and  $15 \text{ yr}^{-1}$  ( $\theta_j = 10^\circ$ ). We find that the HLV network, operating at zero-detuning and high laser power, would shorten these times to 4.9 months ( $\theta_j = 30^\circ$ ) and 17 days ( $\theta_j = 10^\circ$ ), with corresponding event rates of  $5.6 \text{ yr}^{-1}$  and  $49 \text{ yr}^{-1}$ . Alternatively, the binary coalescence model for short GRB progenitors can

be ruled out if an HLV network does not observe a binary within the first two years of observation.

Finally, we have shown that the rate of GRB triggered observations of GW systems associated with GRBs is lower than the rate of untriggered observations if  $\theta_j \gtrsim 30^\circ$ . This result is independent of network, noise curve, and GRB rate, and when coupled with recent observations of small beaming angles for short GRBs, suggests that the first detections of GRB progenitors with advanced GW networks will not involve the observation of GRBs.

We conclude that, assuming short GRBs are the result of the merger of compact objects, and assuming that the resulting gamma-rays are beamed, the first detection of gravitational-waves from binary coalescence associated with a GRB progenitor will be untriggered, and may occur within months of operation of a modest network of ground-based gravitational wave observatories.

We acknowledge valuable discussions with Edo Berger, Laura Cadonati, Curt Cutler, Wen-fai Fong, Peter Shawhan, and Rai Weiss.

#### REFERENCES

- Abadie, J., et al. 2010, *Class. Quantum Grav.*, 27, 173001  
 —. 2011, arXiv:1111.7314  
 —. 2012a, *A&A*, 539, A124  
 —. 2012b, arXiv:1203.2674  
 Abbott, B., et al. 2008, *ApJ*, 681, 1419  
 Belczynski, K., Dominik, M., Bulik, T., et al. 2010, *ApJ*, 715, L138  
 Belczynski, K., Perna, R., Bulik, T., et al. 2006, *ApJ*, 648, 1110  
 Berger, E. 2011, *New A Rev.*, 55, 1  
 Berger, E., Fox, D. B., Price, P. A., et al. 2007, *ApJ*, 664, 1000  
 Bloom, J. S., Holz, D. E., Hughes, S. A., et al. 2009, arXiv:0902.1527  
 Brady, P. R., Creighton, J. D. E., & Wiseman, A. G. 2004, *Classical and Quantum Gravity*, 21, 1775  
 Briggs, M. S., et al. 2012, arXiv:1205.2216  
 Church, R. P., Levan, A. J., Davies, M. B., & Tanvir, N. 2011, *MNRAS*, 413, 2004  
 Coward, D., Howell, E., Piran, T., et al. 2012, arXiv:1202.2179  
 Dalal, N., Holz, D. E., Hughes, S. A., & Jain, B. 2006, *Phys. Rev. D*, 74, 063006  
 Dietz, A. 2011, *A&A*, 529, A97  
 Dominik, M., Belczynski, K., Fryer, C., et al. 2012, arXiv:1202.4901  
 Evans, P. A., et al. 2012, arXiv:1205.1124  
 Fong, W., Berger, E., & Fox, D. B. 2010, *ApJ*, 708, 9  
 Fong, W., Berger, E., Margutti, R., et al. 2012, arXiv:1204.5475  
 Grupe, D., Burrows, D. N., Patel, S. K., et al. 2006, *ApJ*, 653, 462  
 Guetta, D., & Stella, L. 2009, *A&A*, 498, 329  
 Holz, D. E., & Hughes, S. A. 2005, *ApJ*, 629, 15  
 Janka, H.-T., Mazzali, P., Aloy, M.-A., & Pian, E. 2006, *ApJ*, 645, 1305  
 Levan, A. J., Tanvir, N. R., Jakobsson, P., et al. 2008, *MNRAS*, 384, 541  
 Metzger, B. D., & Berger, E. 2012, *ApJ*, 746, 48  
 Nakar, E., Gal-Yam, A., & Fox, D. B. 2006, *ApJ*, 650, 281  
 Nissanke, S., Holz, D. E., Hughes, S. A., Dalal, N., & Sievers, J. L. 2010, *ApJ*, 725, 496  
 Nissanke, S., Sievers, J., Dalal, N., & Holz, D. 2011, *ApJ*, 739, 99  
 O’Shaughnessy, R., Kim, C., Kalogera, V., & Belczynski, K. 2008, *ApJ*, 672, 479  
 Panaitescu, A. 2006, *MNRAS: Letters*, 367, L42  
 Perley, D. A., Metzger, B. D., Granot, J., et al. 2009, *ApJ*, 696, 1871  
 Popham, R., Woosley, S., & Fryer, C. 1999, *ApJ*, 518, 356  
 Rezzolla, L., Giacomazzo, B., Baiotti, L., et al. 2011, *ApJ*, 732, L6  
 Rosswog, S., & Ramirez-Ruiz, E. 2002, *ApJ*, 336, L7  
 Sathyaprakash, B., & Schutz, B. 2009, *Living Rev. Rel.*, 12, 2  
 Schutz, B. F. 1986, *Nature*, 323, 310  
 —. 2011, *Class. Quantum Grav.*, 28, 125023  
 Soderberg, A. M., Berger, E., Kasliwal, M., et al. 2006, *ApJ*, 650, 261